A laser study of the blue electronic transitions of CaS

C. N. Jarman, R. A. Hailey, and P. F. Bernath[a),b)]
Department of Chemistry, University of Arizona, Tucson, Arizona 85721

(Received 30 October 1991; accepted 9 January 1992)

Three new electronic transitions of CaS have been observed in the blue region of the spectrum. The vibrational bands in these transitions span thousands of cm^{-1} owing to a large change in geometry. Approximately 1000 cm^{-1} portion of the spectrum containing these bands has been recorded at high resolution by dye laser excitation spectroscopy and analyzed. The new states all have $\Omega = 1$, and are tentatively labeled $G\,^1\Pi$, $F\,^1\Pi$, and $f\,^3\Pi_1$. Spectroscopic constants have been generated for all three upper states and for the $X\,^1\Sigma^+$ state from a fit to 4340 individual lines. These constants have been used to generate potential curves and Franck–Condon factors.

I. INTRODUCTION

In recent years, the low-lying electronic energy levels of calcium oxide, CaO, have been studied by a variety of spectroscopic techniques.[1–4] These molecular energy levels (except the ground state) are best thought of as arising from a localized ionic model in which there is one e^- in an orbital centered on Ca^+, and one hole in a p orbital centered on O^-. The ground state is formally Ca^{2+} and O^{2-}. Transitions from the ground electronic state ($X\,^1\Sigma^+$) to one of these low-lying electronic states thus involve a formal transfer of an e^- from O^{2-} to Ca^{2+}. Most of the low-lying states of CaO have now been observed experimentally by Field and co-workers (see Refs. 1–4 and references cited therein).

In contrast, the energies of the low-lying electronic states of calcium sulfide, CaS, are still relatively unknown. The only rotational analysis of an electronic transition was performed in 1968 by Blues and Barrow who observed the absorption spectrum of the $A\,^1\Sigma^+$–$X\,^1\Sigma^+$ transition.[5] These authors measured several vibrational bands and obtained a value for ω_e of 462.23 cm^{-1} in the ground state. A later study of CaS in an argon matrix by Martin and Schaber[6] produced a value of 475 cm^{-1} for the fundamental, in general agreement with the previous determination.

The dissociation energy of CaS in the ground electronic state was determined by the mass spectrometric studies of Colin, Goldfinger, and Jeunehomme in 1964.[7] These authors, however, did not have accurate spectroscopic data on which to base their calculation. The value they obtained is corrected and compared to theory in the paper by Partridge, Langhoff, and Bauschlicher.[8] The theoretical value of $D_0 = 3.29(23)$ eV is within one standard deviation of the experimental value of 3.46(20) eV.

The most recent spectroscopic investigation of CaS is the millimeter wave study in the ground electronic state by Takano, Yamamoto, and Saito.[9] These authors measured transitions with $J'' = 18 - 28$ and $v'' = 0 - 3$, and obtained $B_e = 0.176\,675\,665(50)$ cm^{-1}, $\alpha_e = 0.000\,826\,975(73)$ cm^{-1}, and $D_e = 1.032\,017(60) \times 10^{-7}$ cm^{-1}. The motivation for this work was the possibility of the discovery of CaS in dark molecular clouds by radio astronomy.

This paper presents the first high resolution laser study of CaS. The analysis of the blue part of the spectrum resulted in the detection of three new electronic states tentatively labeled $G\,^1\Pi$, $F\,^1\Pi$, and $f\,^3\Pi_1$.

II. EXPERIMENTAL DETAILS AND LOW RESOLUTION SPECTRA

CaS was produced in a conventional Broida oven[10] from the reaction of calcium vapor with OCS. The laser used in this study was a Coherent 699-29 ring dye laser operating with Stilbene 3 dye and pumped by 5 Watts multiline UV radiation from a Coherent Innova 200 argon ion laser. The dye laser beam was chopped with a mechanical chopper, and focused vertically in the flame.

Initially, we scanned the dye laser broadband (~ 1 cm^{-1} resolution), and lock-in detected the total laser induced fluorescence at right angles to the beam with a photomultiplier tube. This spectrum exhibited two long series of vibrational bands between 425 nm and 473 nm (Fig. 1), one much stronger than the other. We inferred from this spectrum that we were seeing fluorescence from two electronic states. Next, we fixed the laser on several strong features, and focused the total fluorescence onto the entrance slits of a 0.64 m monochromator. The dispersed fluorescence was then detected with a photomultiplier tube, processed by photon counting electronics, and recorded on chart paper. Spectra were recorded by scanning the monochromator for each laser position. The most intense resonant feature in all these spectra was a band system centered at 615 nm, which we assign as transitions from the upper electronic state to the $A\,^1\Pi$ state (Fig. 2). (We rename Blues and Barrow's transition[5] as $B\,^1\Sigma^+$–$X\,^1\Sigma^+$.) These spectra also contained nonresonant features between 620 nm and 660 nm, and we attribute these to transitions from many collisionally populated electronic states lower in energy than the state populated by the laser to the $A\,^1\Pi$, $a\,^3\Pi$, and $b\,^3\Sigma^+$ states. The nonresonant emission therefore corresponds to the complex orange band emission of CaO.[1]

a) Camille and Henry Dreyfus Teacher–Scholar.
b) Also: Department of Chemistry, University of Waterloo, Waterloo, Ontario, Canada N2L 3G1.

 0021-9606/92/085571-06$06.00 © 1992 American Institute of Physics

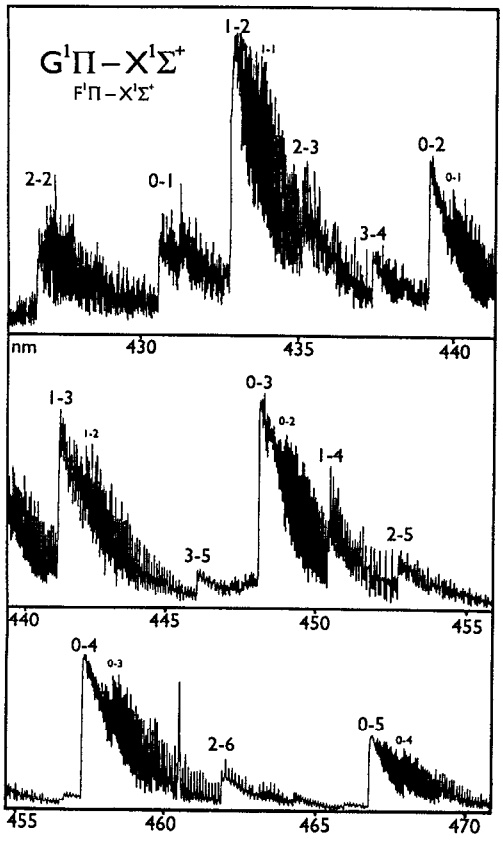

FIG. 1. The low resolution laser excitation spectrum of CaS.

A further low resolution dye laser scan was then performed with a 10 nm bandpass filter centered at 620 nm inserted between the laser beam and the photomultiplier tube. This scan was less noisy than the scan without the filter, but the spectra were identical, and is reproduced in Fig. 1. The large change in geometry is evident both in the extent of the vibrational progressions and in the strong degradation of the rotational structure to longer wavelengths

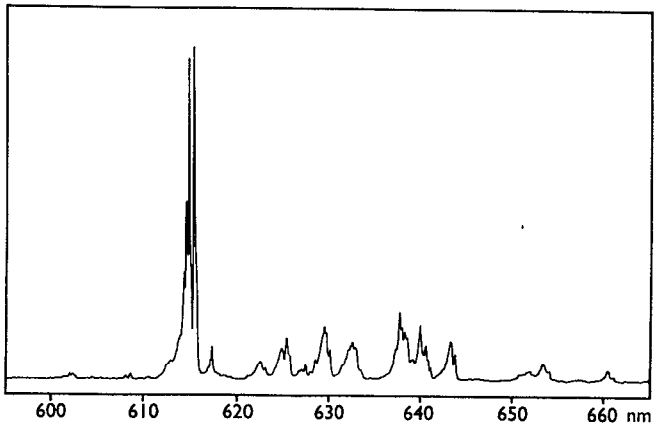

FIG. 2. The dispersed fluorescence spectrum obtained with the laser fixed on the 0–2 head of the $G\,^1\Pi$–$X\,^1\Sigma^+$ transition.

(which indicates an increase in the Ca–S bond length in both excited states).

Following the low resolution survey scans, high resolution (1 MHz laser bandwidth) laser excitation spectra were recorded. All of the high resolution scans were performed with the bandpass filter in place, and the spectra were stored as a function of frequency using Coherent's PC-Autoscan software. The spectrum was recorded at Doppler-limited resolution between 22 450 and 23 430 cm^{-1}. The frequency scale was calibrated by recording the thorium atomic lines using the optogalvanic effect at the beginning and end of each day and comparing these frequencies with the published line list.[11]

III. ANALYSIS OF THE SPECTRUM

The high resolution data files were converted to ASCII format for use with the data reduction package PC-DECOMP developed at the National Solar Observatory by J. W. Brault. Each line in the high resolution spectrum was first fit to a Voigt profile using PC-DECOMP, and then the line positions and intensities were used as input to PC-LOOMIS, an interactive color Loomis–Wood program developed at the University of Arizona by C. N. Jarman. PC-LOOMIS is of great assistance in rapidly picking out branches in complex spectra and is available from the author on request.

The rotational structure of *all* the vibrational features in the spectrum consisted of strong Q branches together with weaker P and R branches, consistent with transitions from $\Omega = 1$ upper electronic states to the ground electronic state. There is a large increase in the Ca–S bond distance ($\Delta B \approx 20\%$ of B), and this causes the R branches to form heads at very low J, and then run concurrently with the Q and P branches. The spacings between adjacent lines are similar in all three branches. Because the low J lines were overlapped in many cases, it was often impossible to distinguish between the P and R branches in the Loomis–Wood program. The correct rotational assignment of these branches (including which was P and which was R) was achieved by using combination differences generated from the rotational constants of $^{40}Ca^{32}S$ in the ground electronic state provided by the millimeter wave study by Takano, Yamamoto, and Saito.[9] In this way, both the rotational and the ground state vibrational quantum numbers were assigned for the majority of the P and R branches. The remaining unassigned P and R branches were found to be due to $^{40}Ca^{34}S$ (4% natural abundance) using rotational constants predicted from the isotope relations. The rotational assignment of the Q branches in each vibrational band was achieved by forcing the Q branch to have the same origin as the P and R branches.

At this point in the analysis, the assignment of the spectrum was complete in all but one area—the vibrational assignment for the two upper electronic states. This assignment was achieved for the electronic state responsible for the most intense fluorescence, by examining the intensities of the resonant vibrational bands in the dispersed fluoresence scans. The large change in internuclear distance means that

TABLE I. Rotational constants for individual vibrational levels in $^{40}Ca^{32}S$ (cm^{-1}).

	v	T_v	B_v	$D_v \times 10^{-7}$	$H_v \times 10^{-11}$	$q_v \times 10^{-3}$	$q_{vD} \times 10^{-7}$	$q_{vH} \times 10^{-11}$
$X^1\Sigma^+$	0	0.000 00	0.176 261 581 1(83)	1.0346 15(65)				
	1	458.670 48(33)	0.175 429 962(10)	1.0400 33(77)				
	2	913.775 51(37)	0.174 593 748(14)	1.0456 82(98)				
	3	1 365.301 40(44)	0.173 752 875(23)	1.0511 0(17)				
	4	1 813.239 08(85)	0.172 905 82(68)	1.0542 5(99)				
	5	2 257.576 00*	0.172 057 1(57)	1.064 6(89)				
	6	2 698.302 0(10)	0.171 204 1(57)	1.074 7(89)				
	7	3 135.405 6(11)	0.170 345 1(61)	1.088(17)				
$G^1\Pi$	0	23 665.230 51(46)	0.144 866 02(32)	1.0813 1(75)	−0.001 63(46)	−0.066 78(21)	0.003 48(25)	
	1	23 998.862 58(50)	0.144 043 56(31)	1.0774 5(71)	−0.002 95(42)	−0.058 57(18)	0.006 06(22)	
	2	24 329.781 16(52)	0.143 220 12(39)	1.069 8(10)	−0.006 14(70)	−0.045 37(27)	0.006 55(37)	
	3	24 657.999 8(10)	0.142 402 78(72)	1.074 9(10)		−0.030 64(53)	0.008 97(85)	
	4	24 983.544 1(10)	0.141 584 56(76)	1.075 4(11)		−0.011 62(52)	0.010 53(88)	
	5	25 306.418 95(75)	0.140 768 1(57)	1.077 7(86)		0.010 31(54)	0.012 1(12)	
	6	25 626.636 91(83)	0.139 953 5(57)	1.077 8(87)		0.034 90(85)	0.014 1(25)	
	7	25 944.211 6(14)	0.139 145 0(59)	1.091(16)		0.066 51(78)		
$F^1\Pi$	0	23 168.612 69(53)	0.147 041 83(64)	1.271 6(16)		0.373 9(17)	−0.257(12)	0.122(22)
	1	23 501.766 73(55)	0.146 214 78(45)	1.274 21(91)		0.407 16(85)	−0.300 7(42)	0.177 3(52)
	2	23 832.313 79(62)	0.145 394 07(54)	1.277 0(10)		0.439 6(12)	−0.303 4(70)	0.154 6(93)
	3	24 160.260 9(24)	0.144 587 1(18)	1.292 8(31)		0.480 2(39)	−0.304(24)	0.114(33)
	4	24 485.634 5(14)	0.143 789 6(30)	1.359(15)		0.539 9(35)	−0.382(24)	
$f^3\Pi_1$	1	23 448.163 23(95)	0.144 917 0(24)	2.508(16)	1.438(30)	2.376 4(25)	−3.005(23)	2.895(47)
	2	23 782.230 7(10)	0.144 217 1(22)	2.657(13)	1.527(23)	2.508 9(28)	−3.372(23)	3.118(43)

*Fixed to the value determined in the Dunham fit.

the structure of the upper state vibrational wave function is reflected in the intensity distribution of the ground state vibrational progressions. For example, if the laser excites $v = 0$ in the upper state, then the ground state fluorescence progression contains no "nodes."

In this way, the upper state vibrational quantum numbers could be assigned for the main isotopomer ($^{40}Ca^{32}S$) of the most intense electronic transition, and the individual rotational lines were then fit to a Hamiltonian which treated each vibration as a separate state. The standard rotational energy level expression

$$F(J) = T + BJ(J+1) - D[J(J+1)]^2 + H[J(J+1)]^3 \pm \frac{\delta_{\Lambda,1}}{2}\{qJ(J+1) + q_D[J(J+1)]^2 + q_H[J(J+1)]^3\}$$

was used. The rotational parameters from this fit are reproduced in Table I. No local or global perturbations were evident, and so we then combined the separate vibrational levels by representing the energy levels of each electronic state with the Dunham expression,

$$F(J,v) = \sum_{l,m} Y_{lm}(v+1/2)^l[J(J+1)]^m \pm \delta_{\Lambda,1}\sum_{l,m} Q_{lm}(v+1/2)^l[J(J+1)]^m.$$

The vibration–rotation parameters Y_{lm} and Q_{lm} obtained from this fit were then used to predict additional vibrational bands which were picked out in PC-LOOMIS, and included in subsequent fits. The final Dunham constants were obtained from a fit which included 2700 transitions between $v = 0 - 7$ and $J = 0 - 114$ in the upper and lower electronic states. The constants are reproduced in Table II, and the line positions are available from the authors on request and in PAPS Ref. 12. Because there was no experimental connection between $v = 4$ and 5 of the ground state, the term energy of $v'' = 5$ reported in Table I was fixed to the value predicted from the final Dunham fit in Table II. Both final fits included the millimeter wave data.[9]

The Dunham constants ($Y_{l0}, Y_{l1}, l = 1 - 4$) were then used to obtain Rydberg–Klein–Rees (RKR) potential curves for the ground and upper electronic states, from which the Franck–Condon factors in Table III were calculated. The observed intensity variations in the low resolution spectra agree well with the predicted Franck–Condon factors assuming a vibrational temperature of about 1000 K. This provided one check on the upper state vibrational assignment. As an additional check, the Dunham constants for $^{40}Ca^{34}S$ were predicted from the isotopic relations, and the line positions predicted. The agreement between prediction and observation was almost perfect, also confirming the vibrational assignment. The $^{40}Ca^{34}S$ lines[12] were then fit to the Dunham equations (Table IV). The lines for the $^{44}Ca^{32}S$ (2% natural abundance) isotopomer were also predicted but proved to be too weak to be seen in the congested spectrum.

The vibrational assignment for the second (weaker) electronic transition could not be determined from the nodal structure in the resolved fluorescence scans, and so we initially assumed that the lowest observed vibrational level cor-

TABLE II. Dunham constants for $^{40}Ca^{32}S$ (in cm^{-1}).

	$X\,^1\Sigma^+$	$G\,^1\Pi$	$F\,^1\Pi$	$f\,^3\Pi_1$
Y_{00}	0.000 00	23 728.061 61(69)	23 231.720 8(11)	23 177.730 2(22)
Y_{10}	462.228 56(50)	336.365 40(85)	335.786 1(24)	334.068 9(11)
Y_{20}	− 1.775 53(15)	− 1.372 39(46)	− 1.324 9(17)	
$Y_{30}\times10^{-2}$	− 0.181 0(12)	0.364 7(95)	0.593(45)	
$Y_{40}\times10^{-3}$		− 0.081 9(63)	− 0.391(40)	
Y_{01}	0.176 675 662(12)	0.145 277 61(27)	0.147 458 46(76)	0.145 976 3(31)
$Y_{11}\times10^{-3}$	− 0.827 033(21)	− 0.824 42(17)	− 0.832 28(39)	− 0.705 0(16)
$Y_{21}\times10^{-5}$	− 0.227 6(13)	0.078 4(28)	0.322 6(66)	
$Y_{31}\times10^{-8}$	− 0.65(22)			
$Y_{02}\times10^{-6}$	− 0.103 179 6(73)	− 0.108 099(49)	− 0.127 93(28)	− 0.236 4(11)
$Y_{12}\times10^{-7}$	− 0.005 540(45)	0.003 80(19)	− 0.005 83(58)	− 0.106 3(44)
$Y_{22}\times10^{-10}$		− 0.347(36)		
$Y_{03}\times10^{-10}$		− 0.000 349(27)	0.001 94(34)	0.147 4(17)
$Q_{01}\times10^{-2}$		− 0.003 632 0(75)	0.018 042(46)	0.110 03(18)
$Q_{11}\times10^{-4}$		0.037 13(41)	0.126 2(26)	0.604 8(96)
$Q_{21}\times10^{-5}$		0.073 91(68)	0.135 7(49)	
$Q_{02}\times10^{-6}$		0.000 284 6(74)	− 0.012 82(21)	− 0.133 70(87)
$Q_{12}\times10^{-7}$			− 0.009 44(43)	− 0.128 8(34)
$Q_{03}\times10^{-10}$			0.007 54(29)	0.150 6(16)
σ		0.0036		0.004 8

responded to $v' = 0$. The rotational lines were then fit to Dunham expressions, and RKR curves were computed from which Franck–Condon factors were calculated. The upper state vibrational assignment was then shifted by one, and new Dunham constants, RKR potential curves, and Franck–Condon factors were calculated. This process was repeated several times to yield different sets of Franck–Condon factors for each vibrational assignment. The correct vibrational assignment was then found by comparing the calculated Franck–Condon factors for each vibrational assignment with the observed intensities of the vibrational bands in the low resolution spectrum. Our initial assignment proved to be correct, with $v' = 0 - 4$. The Franck–Condon factors for this electronic transition are given in Table V. The RKR curves for the ground state and the two excited states are shown in Fig. 3.

After fitting both electronic transitions, and removing these lines in PC-LOOMIS, we were able to pick out some additional vibrational sequence structure for the main isotopomer which did not connect to either of the two upper electronic states. We concluded that we were seeing weak transitions to a third electronic state. Because each band contained *PQR* structure for all values of *J*, we deduced that we were seeing transitions from vibrational levels in an $\Omega = 1$ electronic state. As before, we attempted to assign the vibrational quantum numbers in the upper state by Franck–Condon analysis. Unfortunately, only two upper state vibrational levels were observed, and while we are sure that neither had $v' = 0$, the actual assignment is not certain: we favor $v' = 1$ and 2, but $v' = 2,3$ or $v' = 3,4$ are also possible.

The transitions for both new electronic states were then included in the fit to separate vibrational states (Table I). As it can be seen, the size of the lambda doubling constant q was similar in each electronic state, but different by factors of ~ 5 between electronic states. The Dunham constants for both new electronic states ($v' = 1,2$ for the weak transition), are shown in Table II.

TABLE III. Franck–Condon factors for $G\,^1\Pi$–$X\,^1\Sigma^+$ $^{40}Ca^{32}S$.

v' \ v''	0	1	2	3	4	5	6	7	8
0	0.003	0.018	0.059	0.122	0.178	0.198	0.173	0.123	0.071
1	0.014	0.064	0.129	0.136	0.068	0.005	0.020	0.092	0.147
2	0.036	0.111	0.118	0.035	0.004	0.067	0.092	0.035	0.001
3	0.067	0.124	0.048	0.003	0.068	0.062	0.002	0.034	0.082
4	0.098	0.095	0.002	0.051	0.060	0.001	0.045	0.061	0.004
5	0.120	0.048	0.014	0.070	0.006	0.035	0.053	0.000	0.042
6	0.128	0.011	0.051	0.036	0.011	0.057	0.003	0.037	0.041
7	0.124	0.000	0.068	0.003	0.047	0.019	0.020	0.045	0.000
8	0.110	0.013	0.054	0.008	0.050	0.001	0.049	0.004	0.035

TABLE IV. Dunham constants for $^{40}Ca^{34}S$ (in cm^{-1}).

	$X\,^1\Sigma^+$	$G\,^1\Pi$
Y_{00}		23 728.040 5(55)
Y_{10}	454.663 6(47)	330.752 0(20)
Y_{20}	− 1.732 34(90)	− 1.312 93(63)
Y_{01}	0.170 925 3(84)	0.140 543 4(79)
$Y_{11}\times10^{-3}$	− 0.788 5(17)	− 0.785 67(26)
$Y_{21}\times10^{-5}$	− 0.158 (31)	
$Y_{02}\times10^{-6}$	− 0.097 9(11)	− 0.103 1(10)
$Y_{12}\times10^{-9}$	− 0.71(12)	
$Q_{01}\times10^{-4}$		− 0.335 6(38)
$Q_{11}\times10^{-5}$		0.330(54)
$Q_{21}\times10^{-5}$		0.162(17)
$Q_{02}\times10^{-9}$		0.549(55)
σ	0.0060	

TABLE V. Franck–Condon factors for $F\,^1\Pi$–$X\,^1\Sigma^+$ $^{40}Ca^{32}S$.

v' \ v''	0	1	2	3	4	5	6	7	8
0	0.007	0.038	0.100	0.171	0.207	0.192	0.140	0.083	0.040
1	0.029	0.106	0.155	0.105	0.019	0.008	0.078	0.145	0.151
2	0.068	0.142	0.083	0.001	0.046	0.101	0.054	0.001	0.039
3	0.109	0.115	0.007	0.043	0.084	0.015	0.019	0.083	0.057
4	0.139	0.054	0.014	0.081	0.014	0.026	0.072	0.014	0.018
5	0.148	0.008	0.061	0.039	0.012	0.066	0.008	0.030	0.062
6	0.137	0.002	0.076	0.001	0.057	0.020	0.022	0.054	0.001

IV. ELECTRONIC ASSIGNMENT

Our electronic assignment is based upon the known electronic structure of CaO, in which the sixth and seventh excited states in the singlet and triplet manifolds have Π symmetry (see Fig. 1 of Ref. 1). The spectrum arising from transitions between the lower of these electronic states and the ground electronic state was analyzed by Lagerqvist in 1954.[13] The electronic origin for this state was determined at 25 913.0 cm^{-1}. Because this was the second observed excited state at that time, Lagerqvist labeled it the $B\,^1\Pi$ state. The position of the seventh excited state ($^1\Pi$) was much later determined by Baldwin and Field to be 26 794.711(19) cm^{-1} in the analysis of the green band transitions of CaO,[3] and labeled $F\,^1\Pi$. We label the corresponding states in CaS according to their (presumed) true energy order. Thus the $F\,^1\Pi$ and $G\,^1\Pi$ states of CaS correlate with the $B\,^1\Pi$ and $F\,^1\Pi$ states in CaO, respectively. The labeling of the triplet states remains unchanged.

We have observed transitions from three new $\Omega = 1$ electronic states of CaS in the blue region of the spectrum. The vibrational assignment of the two highest electronic states is certain, and places one state $\sim$496 cm^{-1} above the other. Transitions to the third electronic state are much weaker, and only two vibrational levels have been observed. The tentative assignment from the Franck–Condon analysis put the state $\sim$54 cm^{-1} below the lower of the two highest states. Because the vibrational assignment is not secure, the third state could also lie $\sim$388 or $\sim$722 cm^{-1} lower. Transitions from the highest state to the ground state are extremely intense, and so it is clear that this state has singlet character. The presence of strong Q branches and weaker PR structure indicates that this state is either the $F\,^1\Pi$ or the $G\,^1\Pi$.

Initially, we assigned the highest state as the $F\,^1\Pi$, and the next lowest state as the $f\,^3\Pi_1$ state arising from the same $A\pi\sigma^{-1}$ electronic configuration. This unfortunately left the third $\Omega = 1$ state without a convincing assignment, although high v's of $e\,^3\Sigma_1^-$ or of $d\,^3\Delta_1$ were possible. This assignment also required the singlet–triplet splitting in the $A\pi\sigma^{-1}$ configuration to be $\sim$496 cm^{-1}. The corresponding energy gap in CaO has not been determined experimentally, but is predicted to be small because the exchange integrals which are responsible for separating the energies of the $F\,^1\Pi$ and the $f\,^3\Pi$ states couple molecular orbitals localized on Ca^{2+} to molecular orbitals localized on O^{2-}.[14] This energy difference therefore seemed too large for our initial assignment, and was more comparable to the observed $\sim$882 cm^{-1} energy separation between the $B\,^1\Pi$ and $F\,^1\Pi$ states in CaO, allowing for a decrease in the separation on substituting sulfur for oxygen (larger internuclear distance). Thus we assign the highest state as the $G\,^1\Pi$, and the next lowest state as the $F\,^1\Pi$ state. Such an assignment also allows the third state to be assigned as the $f\,^3\Pi_1$ state. For the vibrational assignment we preferred, this sets the singlet–triplet splitting in the $A\pi\sigma^{-1}$ configuration at $\sim$54 cm^{-1}, more in line with what we expected. All the figures and tables in this paper have been labeled with this second assignment. However, it must be stressed that this is only the electronic assignment we favor—it is possible that our initial assignment is correct, although less likely.

We have assigned the resonant feature at 615 nm in the dispersed fluorescence spectrum (Fig. 2) as the $G\,^1\Pi$–$A\,^1\Pi$ electronic transition. Such an assignment places the $A\,^1\Pi$ state $\sim$16 260 cm^{-1} below the $G\,^1\Pi$ origin, i.e., $\sim$7470 cm^{-1} above the ground state. This value agrees well with the *ab-initio* value of 6901 cm^{-1} calculated at the singly and doubly excited configuration interaction (SDCI) level of theory by Partridge, Langhoff, and Bauschlicher,[8] and is the basis for our assignment. No attempt has been made to assign the nonresonant features in this spectrum, and we anticipate that sub-Doppler techniques will be needed to perform rotational analyses of these bands.

Perhaps the most interesting aspect of the electronic structure of CaS is the comparison with the isovalent molecule CaO. Unfortunately, the experimental data is too sparse to draw any firm conclusions. Additional experiments are needed to determine the spectroscopic constants for the many missing states. Some additional theoretical work on the excited states of CaS would be most welcome.

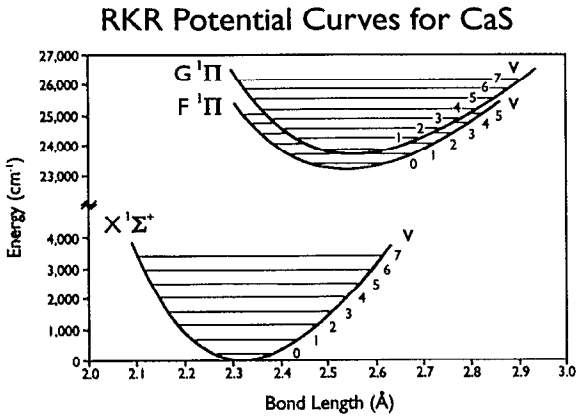

FIG. 3. The RKR potential curves for $X\,^1\Sigma^+$, $F\,^1\Pi$, and $G\,^1\Pi$ states of CaS.

ACKNOWLEDGMENTS

This work was supported by the National Science Foundation (Grant No. CHE-8913785). Partial support was also provided by the NASA Origins of the Solar System Research Program and the Natural Sciences and Engineering Research Council of Canada. We thank R. W. Field for his comments.

[1] J. B. Norman, K. J. Cross, H. S. Schweda, M. Polak, and R. W. Field, Mol. Phys. **66**, 235 (1989).
[2] D. P. Baldwin, J. B. Norman, R. A. Stoltz, A. Sur, and R. W. Field, J. Mol. Spectrosc. **139**, 29 (1990).
[3] D. P. Baldwin and R. W. Field, J. Mol. Spectrosc. **139**, 68 (1990).
[4] D. P. Baldwin and R. W. Field, J. Mol. Spectrosc. **139**, 77 (1990).
[5] R. C. Blues and R. F. Barrow, Trans. Faraday Soc. **65**, 646 (1969).
[6] T. P. Martin and H. Schaber, Spectrochim. Acta A **38**, 655 (1982).
[7] R. Colin, P. Goldfinger, and M. Jeunehomme, Trans. Faraday Soc. **60**, 306 (1964).
[8] H. Partridge, S. R. Langhoff, and C. W. Bauschlicher, Jr., J. Chem. Phys. **88**, 6431 (1988).
[9] S. Takano, S. Yamamoto, and S. Saito, Chem. Phys. Lett. **159**, 563 (1989).
[10] J. B. West, R. S. Bradford, J. D. Eversole, and C. R. Jones, Rev. Sci. Instrum. **46**, 164 (1975).
[11] B. A. Palmer and R. Engleman, Jr., *Atlas of the Thorium Spectrum* Los Alamos National Labs, 9615 (1983).
[12] See AIP document no. PAPS JCPSA-96-5571-30 for 30 pages of tables. Order by PAPS number and journal reference from American Institute of Physics, Physics Auxiliary Publication Service, 335 East 45th Street, New York, NY 10017. The price is $1.50 for each microfiche (60 pages) or $5.00 for photocopies of up to 30 pages, and $0.15 for each additional page over 30 pages. Airmail additional. Make checks payable to the American Institute of Physics.
[13] A. Lagerqvist, Ark. Fys. **8**, 83 (1954).
[14] C. W. Bauschlicher, Jr. and D. R. Yarkony, J. Chem. Phys. **68**, 3990 (1978).